# Influence of Al Content on Oxidation Resistance of Phase-pure Ti₂AlC under Simulated Loss-of-coolant Accident Conditions

LEI Yiming[1,2], ZHANG Jie[1], BAI Guanghai[3], ZHANG Yanwei[3], WANG Xiaohui[1], WANG Jingyang[1]

(1. Shenyang National Laboratory for Materials Science, Institute of Metal Research, Chinese Academy of Sciences, Shenyang 110016, China; 2. School of Materials Science and Engineering, University of Science and Technology of China, Shenyang 110016, China; 3. Life Management Technology Center, Suzhou Nuclear Power Research Institute, China Nuclear Power Technology Research Institute, Suzhou 215004, China)

**Abstract:** To tailor Ti₂AlC coatings for the applications in accident tolerant fuels, the oxidation of near-stoichiometric and Al-lean Ti₂AlC was investigated in Ar-41% H₂O atmosphere in 1000–1200 ℃. The oxidation kinetics of phase-pure Ti₂AlC in high-temperature water vapor varied from parabolic to linear rate law with Al content decreasing. Insufficient Al content could not sustain the growth of continuous alumina scales, resulting in formation of thick unprotective TiO₂-based scales. The formation of thin and protective Al₂O₃ scale for Ti₂AlC with stoichiometric composition effectively inhibited the inward diffusion of water vapor. For the application of protective coatings on Zr-based cladding, stoichiometric Ti₂AlC is expected to protect cladding from fast oxidation and improve the accident tolerance in the current light water reactors.

**Key words:** accident tolerant fuels; Ti₂AlC; water vapor high-temperature oxidation

The development of accident tolerant fuel (ATF) have been launched worldwide to enhance accident tolerance in light water reactors[1-2]. ATFs, in comparison with the standard UO₂-Zr system, can provide larger safety margins by reducing the oxidation rate of Zr-based alloy cladding in high temperature water vapor and increasing the coping time after a loss of coolant accident (LOCA) scenario. In a design-basis LOCA, the maximum oxidation allowed to the zirconium alloy is 17% of the tube wall thickness, which takes 20 min at 1100 ℃ and only 8 min at 1200 ℃[3]. A prospective solution is the substitution of Zr alloys with advanced cladding materials or use of protective coatings, which is meant to provide short-term additional protection to the zirconium alloy cladding at high temperature. Surface-modified zircaloy cladding are regarded as a competitive concept with the merits of convenience and economics[4-5].

The basic prerequisite requirement of coating candidates for ATF is their resistance to high-temperature water vapor oxidation. Up to now, Cr-coated cladding was reported to perform good high temperature water vapor oxidation resistance, owing to the formation of a protective Cr₂O₃ scales[6-7]. Al-containing MAX phase, especially Ti₂AlC, is considered as another promising candidate, which exhibits outstanding oxidation resistance at high temperature, due to the formation of a dense and adherent Al₂O₃ scale[8-10]. Under water vapor containing environment, Al₂O₃ shows higher stability, for instance, the weight loss rate is two orders of degree lower than that of Cr₂O₃ at 1200 ℃[11-12]. However, it is challenging for Ti₂AlC coating to obtain a continuous and compact Al₂O₃ layer during the oxidation process and therefore maintain the same high temperature oxidation resistance as bulk materials. Tang et al.[13] demonstrated that magnetron sputtered TiC/Ti₂AlC coating can provide sufficient protection of the Zry-4 alloy at 800 ℃ for 150 min, and multilayer oxide scale (Al₂O₃+TiO₂/Al₂O₃/TiO₂) was observed after oxidation. The formation of triple oxide structure was also reported by Li et al.[14] for post-annealed Ti₂AlC coating after oxidation at 1000 and 1200 ℃, which can be attributed to the loss of Al content for inward diffusion during the oxidation. The chemical composition, especially Al content in Ti₂AlC, influences the phase composition and structure of the oxide scale

formed on ceramic. Li *et al.*[15] reported that the sufficient outward flux of Al was necessary for the steady growth of alumina scale on $Ti_3AlC_2$ at high temperature. Thus, the performance of $Ti_2AlC$ with specific Al content during a hypothetical LOCA scenario should be clarified. It was reported that defective $Ti_2AlC$ can sustain phase stability with the ability to accommodate Al vacancies[16]. $Ti_2Al_{0.87}C$ coating was obtained by cathodic arc evaporation, while minority content of TiC was apparent when Al content further decreased. Frodelius *et al.*[17] yielded a film stoichiometry of $Ti_2Al_{0.8}C$ by magnetron sputtering, which enabled the growth of both $Ti_2AlC$ and TiC. Thus, $Ti_2Al_{0.87}C$ exhibits the lowest Al content in the single-phase $Ti_2AlC$ coating. In this work, near-stoichiometric $Ti_2Al_{1.02}C$ and Al-lean $Ti_2Al_{0.88}C$ are synthesized, and the kinetic rate law for water vapor oxidation of $Ti_2AlC$ material in 1000–1200 ℃ is investigated. The influence of Al content on the oxidation mechanism of single-phase $Ti_2AlC$ is further discussed, which can provide an instruction to the design of protective coating for the applications in ATFs.

# 1 Experimental

In this study, fully dense pellets including near-stoichiometric and Al-lean titanium aluminum carbides were synthesized by hot pressing at 1400 ℃. The mixing ratio for Ti, Al and C elemental powders was set as 2.00 : 1.05 : 1.00 and 2.00 : 0.90 : 1.00, aiming at achieving near-stoichiometric and Al-lean $Ti_2AlC$ ceramics, respectively. Detailed description of the synthesis process could be found in previous literature[18]. The specimen with dimension of 10 mm×10 mm×1 mm was cut from the as-sintered bulk pellet, then ground to 2000 grit SiC paper, polished to a 1 μm finish and degreased in acetone. Continuous weight change of $Ti_2AlC$ with two Al contents oxidized in water vapor at 1000–1200 ℃ was monitored by Setsys evolution TGA (Setaram, France) with an accuracy of ±4×10^{-7} g. Specimens were suspended by Pt wire and heated to the desired temperatures at a rate of 15 ℃·min^{-1}. Water vapor was generated by an automated wet gas generator, Wetsys (Setaram, France). Ar-41% $H_2O$ (41 kPa water vapor with Ar) atmosphere was maintained to simulate LOCA condition, and the entire experimental setup was heated above the dew point of the corresponding humidity level.

The Al content in the $Ti_2AlC$ pellets was quantitatively measured by electron probe micro-analyzed (EPMA, EPMA-1610, Shimadzu, Kyoto, Japan). The phase composition of as-synthesized and oxidized samples was identified by X-ray diffraction (XRD) with Cu Kα radiation (Rigaku D/max 2400, Japan). SUPRA 35 scanning electron microscope (SEM, LEO, Oberkochen, Germany) equipped with an energy-dispersive spectroscope (EDS) was used for the surface and cross section microstructure observation.

# 2 Results and discussion

The chemical composition of two as-synthesized bulk pellets is shown in Table 1. Al atomic content is determined to be (25.61±0.60)% and (22.42±0.86)% for near-stoichiometric and Al-lean samples, respectively. Compared with the as-mixed powders, approximately 3% loss of Al content is detected, which is attributed to the evaporation of aluminum during the sintering process[19]. Consequently, near-stoichiometric and Al-lean samples are formulated as $Ti_2Al_{1.02}C$ and $Ti_2Al_{0.88}C$, respectively. Fig. 1 shows the XRD patterns of as-synthesized bulk pellets with two different Al contents. In both cases, $Ti_2AlC$ (PDF#29-0095) is the only phase detected, and no extra peaks are apparent. The characteristic diffraction peaks of $Ti_2Al_{1.02}C$ near-stoichiometric sample (002) planes located at around $2\theta$=12.94°, and the lattice constant *c* of near-stoichiometric sample is determined to be 1.367 nm, which is close to 1.362 nm as reported for stoichiometric $Ti_2AlC$ in previous literature[9, 20-21]. With the Al content decreasing, XRD peaks shift to the higher angle, indicating that Al-lean sample exhibits a decreased lattice constant *c* of 1.358 nm. According to the correlation between Al content and lattice parameters characterized by Wang *et al.*[16], lattice parameter *c* for Al-lean sample is estimated to be 1.356 nm, which agrees well with our results. Moreover, lattice constant *a* remains unchanged for $Ti_2AlC$ with two different Al contents. $Ti_2AlC$ can be described as an alternate stacking of $Ti_2C$ and Al atomic planes along the *c* direction, and the lattice constant *a* is dominated by the $Ti_2C$ slab, which is stable and less disturbed by Al content[16].

The oxidation behavior of near-stoichiometric and Al-lean samples in Ar-41% $H_2O$ atmosphere was studied at 1000–1200 ℃ to evaluate the oxidation resistance

**Table 1   Elemental composition of near-stoichiometric and Al-lean samples**

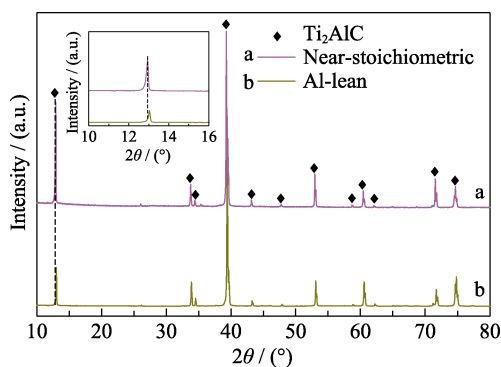| Sample | Atomic percent of Ti/% | Atomic percent of Al/% | Atomic percent of C/% | Composition |
|---|---|---|---|---|
| Near-stoichiometric | (50.25±0.19) | (25.61±0.60) | (24.13±0.61) | $Ti_2Al_{1.02}C$ |
| Al-lean | (50.68±0.19) | (22.42±0.86) | (25.90±0.67) | $Ti_2Al_{0.88}C$ |

Fig. 1   XRD patterns of near-stoichiometric and Al-lean samples

under LOCA conditions. In the experimental atmosphere, the measured weight gain of Zry-4 alloys is close to the predictions by Cathcart-Pawel (C-P) model, which is proposed to describe the oxidation behavior of Zircaloys in hypothetical LOCA scenario[22]. Fig. 2(a) shows the weight gain per unit surface area as a function of time for $Ti_2AlC$ with two different Al contents at 1200 ℃, and the weight gain of Zry-4 alloy is also presented for comparison. The mass gain of $Ti_2Al_{0.88}C$ and $Ti_2Al_{1.02}C$ is 1269 and 27 mg/dm², respectively, which decreases by a factor of three and two orders of magnitude compared to that of Zry-4 alloy (4167 mg/dm²). Fig. 2(b-d) shows the oxidation kinetics of Al-lean and near-stoichiometric samples oxidized at 1000, 1100 and 1200 ℃. Al-lean

sample follows the linear rate law, indicating that the rate-limiting step is the reaction between $Ti_2Al_{0.88}C$ and water vapor. The continuous oxidation during its exposure in high-temperature water vapor results in relatively large weight gains. While oxidation kinetics for near-stoichiometric sample obeys parabolic law. According to the Wagner's theory[23], the scales on $Ti_2Al_{1.02}C$ are protective to the underlying substrate from further oxidation, and the rate-limiting mechanism is diffusion controlled. Different oxidation mechanism is described for $Ti_2AlC$ bulk ceramics with two Al contents, and near-stoichiometric sample shows better oxidation resistance.

It is worth noting that Zry-4 alloys and $Ti_2Al_{1.02}C$ both follow parabolic rate law in high-temperature water vapor oxidation. The parabolic rate constants in Ar-$H_2O$ of various candidate coating and cladding materials[18,24-26] for accident tolerant fuels are summarized in Fig. 3. Compared with Zry-4 alloy, the parabolic rate constant of $Ti_2Al_{1.02}C$ is four orders of magnitudes lower than 1200 ℃. Bare cladding possesses the highest oxidation rate in water vapor, and the slowest rate is measured for SiC. The oxidation rate of $Ti_2Al_{1.02}C$ is between 310SS ($Cr_2O_3$ scale) and alumina-forming FeCrAl alloy APMT (Advanced Powder Metallurgy Tube). We can reasonably conclude that near-stoichiometric $Ti_2AlC$ is a promising candidate to protect Zry-4 cladding from high temperature
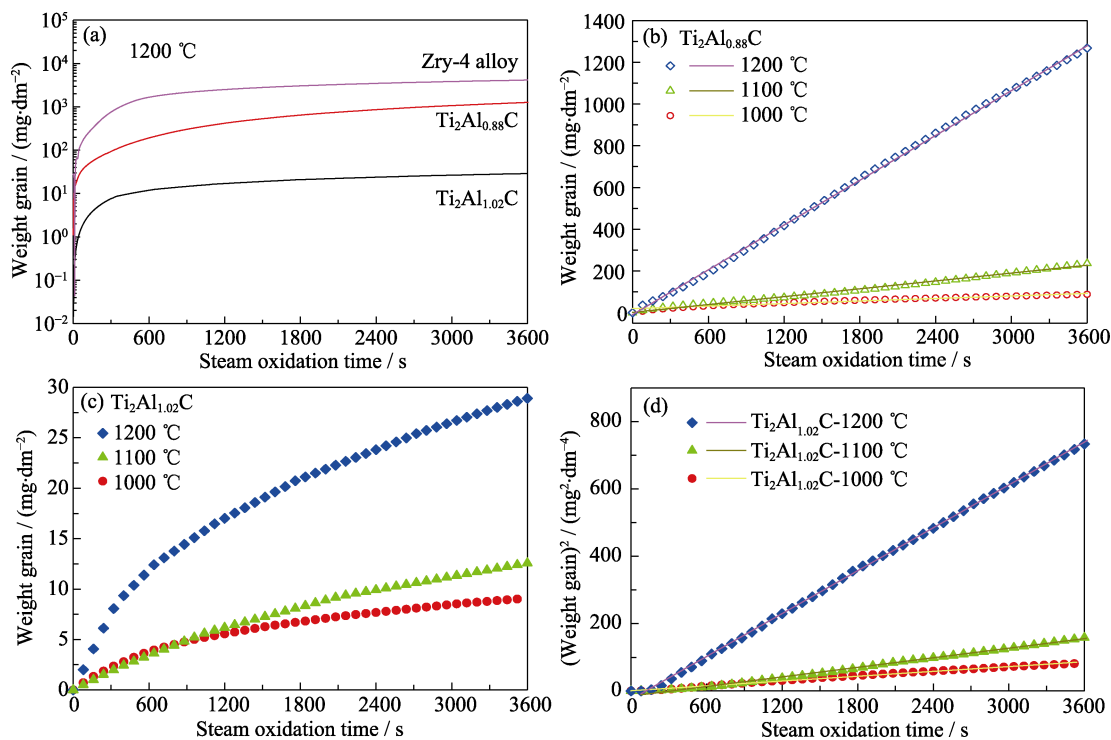


Fig. 2   Weight gain per unit surface area as a function of oxidation time for (a) Zr cladding, Al-lean and near-stoichiometric samples oxidized at 1200 ℃, (b) Al-lean sample at 1000–1200 ℃ and (c) near-stoichiometric sample at 1000–1200 ℃,

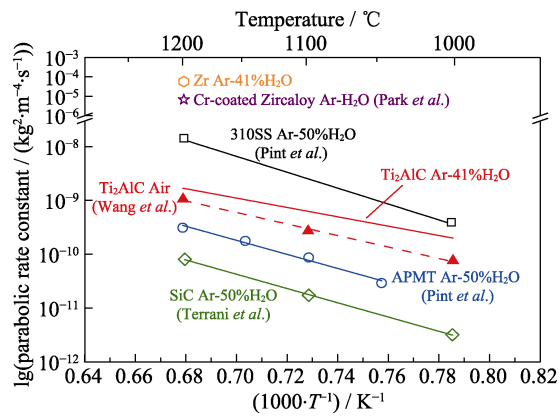and (d) square of weight gain per unit surface area of near-stoichiometric sample as a function of oxidation time

Fig. 3 Arrhenius plot of the high temperature oxidation rate constants for various candidate materials in air and water vapor[18, 24-26]



Fig. 4 XRD patterns of (a) near-stoichiometric and (b) Al-lean samples after oxidation at 1000–1200 ℃

water vapor oxidation. Compared to the air oxidation, oxidation in Ar-41% $H_2O$ atmosphere of $Ti_2Al_{1.02}C$ slightly accelerated. The obtained parabolic rate constant in water vapor at 1200 ℃ is $2.1\times10^{-9}$ $kg^2\cdot m^{-4}\cdot s^{-1}$, which is slightly higher than that in air ($1.1\times10^{-9}$ $kg^2\cdot m^{-4}\cdot s^{-1}$) as reported by Wang et al.[18]. Basu et al.[27] investigated the long-term oxidation of $Ti_2AlC$ in air and 100% water vapor from 1000 to 1300 ℃, and the slightly higher oxidation kinetic for hydrothermal oxidation mainly related to the diffusion of hydroxyl ions with smaller size and lower charge compared to oxide ion through the oxide scale.

In order to reveal the origin of difference in oxidation behaviors of near-stoichiometric and Al-lean samples, phase composition of the oxide scales formed after isothermal oxidation was analyzed by XRD. As illustrated in Fig. 4, in the temperature range of 1000–1200 ℃, the scales formed on near-stoichiometric and Al-lean samples only consist of $TiO_2$ (PDF#21-1276) and $\alpha$-$Al_2O_3$ (PDF#46-1212). The relatively high intensity of diffraction from $Ti_2Al_{1.02}C$ indicates that the oxide scale formed on near-stoichiometric sample is pretty thin, as shown in Fig. 4(a). The intensity of diffraction peaks associated with $Al_2O_3$ increases with oxidation temperature increasing, whereas that for $TiO_2$ remains nearly constant. The scales on near-stoichiometric sample are mainly composed of $Al_2O_3$, with a little of $TiO_2$. For oxidized Al-lean sample (Fig. 4(b)), the intensity of $Ti_2Al_{0.88}C$ is apparently weaker than that of $Ti_2Al_{1.02}C$, revealing thicker oxide scales. With the increase of oxidation temperature, the diffraction peak of $Ti_2Al_{0.88}C$ is further reduced, accompanied with the enhanced diffraction peak of $TiO_2$, indicating thick $TiO_2$-rich oxide scale forms on Al-lean sample after oxidation. The quick growth of $TiO_2$-based scale is non-protective for further oxidation of Al-lean sample, and better oxidation resistance of near-stoichiometric sample can be attributed
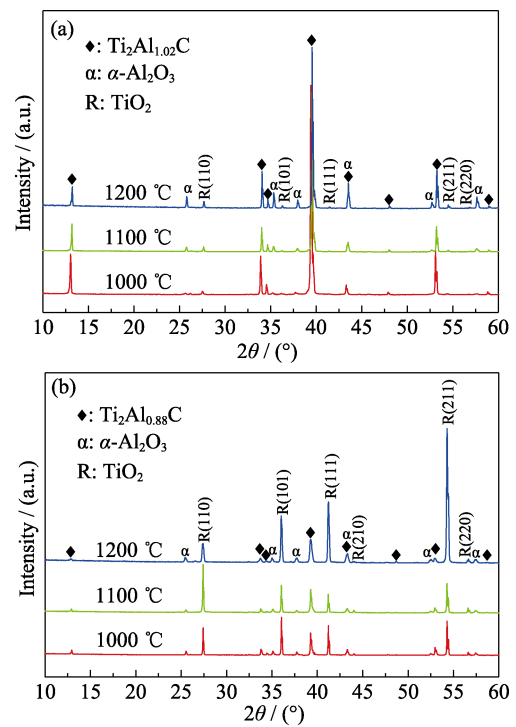
to the formation of a protective $\alpha$-$Al_2O_3$ scale.

Furthermore, SEM observations were conducted to study the morphology of oxidation products on $Ti_2AlC$ bulk ceramics with two different Al contents. Typical surface and cross section morphologies of Al-lean and near-stoichiometric samples after oxidation at 1200 ℃ are shown in Fig. 5. On the surface of Al-lean sample, island colonies of a bright phase are observed, which are the aggregation of large faceted $TiO_2$ grains as evidenced by the insert figure, and the remaining surface is covered by darker $Al_2O_3$ grains. As observed in Fig. 5(b), the oxide scale demonstrates a double-layered structure: the outer scale is solely $TiO_2$ whereas the inner scale is a mixture of $Al_2O_3$ and $TiO_2$. $Al_2O_3$-rich zone is observed at the interface between oxide and $Ti_2Al_{0.88}C$ substrate. For near-stoichiometric sample, isolated islands with large elongated $TiO_2$ grains are embedded in small $Al_2O_3$ grains (Fig. 5(c)). Dense and continuous $Al_2O_3$ scale is clearly detected in Fig. 5(d). The thickness of $Al_2O_3$ scales formed on near-stoichiometric sample is only 2.1 μm, which is two orders of magnitude thinner than that of $TiO_2$-based scale (~180 μm thickness) on the Al-lean sample. The formation of oxide scale on bulk $Ti_2AlC$ with different Al contents is directly influenced by thermodynamics and kinetic aspects[8-9,16,28]. From a thermodynamic point of view, Al has larger tendency for oxidation than Ti. Kinetically, Al atoms have a high diffusivity due to unique structure of $Ti_2AlC$, in which the rigid Ti–C octahedra is weakly coupled by planar Al
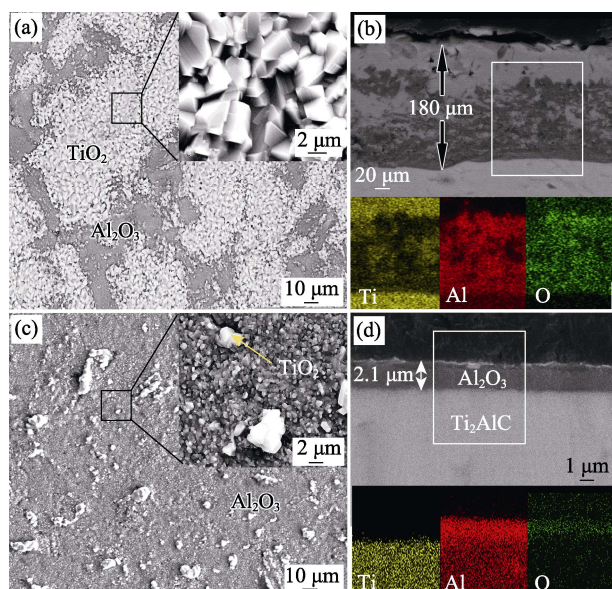
Fig. 5　Typical surface and cross section morphologies of (a, b) Al-lean and (c, d) near-stoichiometric samples after oxidation at 1200 ℃

atomic layers. The formation of $Al_2O_3$ takes place at oxide/substrate interface from inward diffusion of hydroxide ions through the outer oxide layer, and the growth of $TiO_2$ occurs on the outmost surface controlled by outward diffusion of Ti. Basically, more $Al_2O_3$ nuclei than $TiO_2$ is expected on titanium aluminum carbide. With a reduction in Al content, larger alumina grains are needed for the formation of a continuous $Al_2O_3$ scale, which is ultimately hindered by $TiO_2$ grains, owing to the much higher growth velocity. Herein, $TiO_2$-based scales and continuous $Al_2O_3$ scales are formed on near-stoichiometric and Al-lean samples, respectively. The formation of continuous $Al_2O_3$ scales inhibits export of reactants, thereby further oxidation of Ti₂AlC substrate decreasing.

For the application of Ti₂AlC coatings on Zircaloy cladding, thinner coating (10–30 μm) with improved oxidation resistance is needed to reduce neutron absorption and thermal resistance[28]. For stoichiometric Ti₂AlC, the oxide scale growth is dominated by the formation of $\alpha$-$Al_2O_3$ (with a density of 3.98 g/cm³). The oxidation kinetics is parabolic for the growth of a compact $Al_2O_3$ scale controlled by diffusion of hydroxide ions through the oxide scale, and the growth rate constant is calculated to be $9.0 \times 10^{-4}$ μm²·s⁻¹. The oxide scale thickness derived from the weight data is in good agreement with that detected in cross section morphology. By the formation of thin $Al_2O_3$ scales, notably 2.1 μm after oxidation at 1200 ℃ for 1 h, stoichiometric Ti₂AlC offers protection against high-temperature oxidation attack during a hypothetical LOCA scenario.

# 3　Conclusions

In this study, the oxidation behavior of near-stoichiometric (Ti₂Al₁.₀₂C) and Al-lean (Ti₂Al₀.₈₈C) samples were investigated in Ar-41% $H_2O$ atmosphere at 1000–1200 ℃. Near-stoichiometric sample exhibited excellent oxidation resistance, with the parabolic rate constant four orders of magnitude lower than that of Zry-4 at 1200 ℃, owing to the formation of thin and protective $Al_2O_3$ scale. While thick unprotective duplex $TiO_2$-based oxide scales were formed on Al-lean sample, because Al content was insufficient to sustain the growth of continuous alumina scales. The oxidation resistance of titanium aluminum carbide is sensitive to Al content, and stoichiometric Ti₂AlC coating is a promising candidate to protect Zry-4 cladding in the current light water reactors.

## References:

[1]　TERRANI K A. Accident tolerant fuel cladding development: promise, status, and challenges. *Journal of Nuclear Materials*, 2018, **501:** 13–30.

[2]　ZINKLE S J, TERRANI K A, GEHIN J C, *et al*. Accident tolerant fuels for LWRs: a perspective. *Journal of Nuclear Materials*, 2014, **448(1):** 374–379.

[3]　REBAK R B. Accident Tolerant Materials for Light Water Reactor Fuels, 1st edition. Netherlands: Elsevier, 2020**:** 63–81.

[4]　DUAN Z, YANG H, SATOH Y, *et al*. Current status of materials development of nuclear fuel cladding tubes for light water reactors. *Nuclear Engineering and Design*, 2017, **316:** 131–150.

[5]　KIM H G, KIM I H, JUNG Y I, *et al*. Out-of-pile performance of surface-modified Zr cladding for accident tolerant fuel in LWRs. *Journal of Nuclear Materials*, 2018, **510:** 93–99.

[6]　KIM H G, KIM I H, JUNG Y I, *et al*. Adhesion property and high-temperature oxidation behavior of Cr-coated Zircaloy-4 cladding tube prepared by 3D laser coating. *Journal of Nuclear Materials*, 2015, **465:** 531–539.

[7]　BRACHET J C, IDARRAGA T I, FLEM M L, *et al*. Early studies on Cr-Coated Zircaloy-4 as enhanced accident tolerant nuclear fuel claddings for light water reactors. *Journal of Nuclear Materials*, 2019, **517:** 268–285.

[8]　TALLMAN D J, ANASORI B, BARSOUM M W. A critical review of the oxidation of Ti₂AlC, Ti₃AlC₂ and Cr₂AlC in air. *Materials Research Letters*, 2013, **1(3):** 115–125.

[9]　WANG X H, ZHOU Y C. Layered machinable and electrically conductive Ti₂AlC and Ti₃AlC₂ ceramics: a review. *Journal of Materials Science & Technology*, 2010, **26(5):** 385–416.

[10]　NIU Y, FU S, ZHANG K, *et al*. Synthesis, microstructure, and properties of high purity Mo₂TiAlC₂ ceramics fabricated by spark plasma sintering. *Journal of Advanced Ceramics*, 2020, **9(6):** 759–768.

[11]　OPILA E, JACOBSON N, MYERS D, *et al*. Predicting oxide stability in high-temperature water vapor. *The Journal of The Minerals, Metals & Materials Society*, 2006, **58:** 22–28.

[12]　OPILA E, MYERS D. Alumina volatility in water vapor at elevated temperatures. *Journal of the American Ceramic Society*, 2003, **87(9):** 1701–1705.

[13]　TANG C, STEINBRUECK M, STUEBER M, *et al*. Deposition,

characterization and high-temperature steam oxidation behavior of single-phase Ti₂AlC-coated Zircaloy-4. *Corrosion Science*, 2018, **135:** 87–98.

[14] LI W, WANG Z, SHUAI J, *et al*. A high oxidation resistance Ti₂AlC coating on Zirlo substrates for loss-of-coolant accident conditions. *Ceramics International*, 2019, **45(11):** 13912–13922.

[15] LI X, QIAN Y, ZHENG L, *et al*. Determination of the critical content of Al for selective oxidation of Ti₃AlC₂ at 1100℃. *Journal of the European Ceramic Society*, 2016, **36(14):** 3311–3318.

[16] WANG J, ZHOU Y, LIAO T, *et al*. A first-principles investigation of the phase stability of Ti₂AlC with Al vacancies. *Scripta Materialia*, 2008, **58(3):** 227–230.

[17] FRODELIUS J, EKLUND P, BECKERS M, *et al*. Sputter deposition from a Ti₂AlC target: process characterization and conditions for growth of Ti₂AlC. *Thin Solid Films*, 2010, **518(6):** 1621–1626.

[18] WANG X, ZHOU Y. High-temperature oxidation behavior of Ti₂AlC in air. *Oxidation of Metals*, 2003, **59:** 303–320.

[19] ZHU J, QI G, WANG F, *et al*. Effect of aluminum content on synthesis of Ti₂AlC and Ti₃AlC₂ during treatment in a high-energy mill and hot pressing. *Metal Science and Heat Treatment*, 2011, **53(1):** 45–48.

[20] WANG Z, SUN J, XU B, *et al*. Reducing the self-healing temperature of Ti₂AlC MAX phase coating by substituting Al with Sn. *Journal of the European Ceramic Society*, 2020, **40(1):** 197–201.

[21] LIN Z J, ZHUO M J, ZHOU Y C, *et al*. Microstructural characterization of layered ternary Ti₂AlC. *Acta Materialia*, 2006, **54(4):** 1009–1015.

[22] PAWEL R E. The kinetics of oxidation of Zircaloy-4 in steam at high temperatures. *Journal of The Electrochemical Society*, 1979, **126(7):** 1105.

[23] WAGNER C. Theoretical analysis of the diffusion processes determining the oxidation rate of alloys. *Journal of The Electrochemical Society*, 1952, **99(10):** 369.

[24] PARK J H, KIM H G, PARK J Y, *et al*. High temperature steam-oxidation behavior of arc ion plated Cr coatings for accident tolerant fuel claddings. *Surface and Coatings Technology*, 2015, **280:** 256–259.

[25] PINT B A, TERRANI K A, BRADY M P, *et al*. High temperature oxidation of fuel cladding candidate materials in steam–hydrogen environments. *Journal of Nuclear Materials*, 2013, **440(1):** 420–427.

[26] TERRANI K A, PINT B A, PARISH C M, *et al*. Silicon carbide oxidation in steam up to 2 MPa. *Journal of the American Ceramic Society*, 2014, **97(8):** 2331–2352.

[27] BASU S, OBANDO N, GOWDY A, *et al*. Long-term oxidation of Ti₂AlC in air and water vapor at 1000–1300 ℃ temperature range. *Journal of The Electrochemical Society*, 2011, **159(2):** C90–C96.

[28] YOUNKER I, FRATONI M. Neutronic evaluation of coating and cladding materials for accident tolerant fuels. *Progress in Nuclear Energy*, 2016, **88:** 10–18.

# Al 含量对 Ti₂AlC 在核反应堆失水事故下抗氧化性能的影响

雷一明[1,2], 张 洁[1], 柏广海[3], 张晏伟[3], 王晓辉[1], 王京阳[1]

(1. 中国科学院 金属研究所, 沈阳材料科学国家研究中心, 沈阳 110016; 2. 中国科学技术大学 材料科学与工程学院, 沈阳 110016; 3. 苏州热工研究院有限公司 电站寿命管理技术中心, 苏州 215004)

**摘 要:** 为了完善 Ti₂AlC 涂层在事故容错燃料中的设计与应用, 研究了近化学计量比和 Al 含量不足的 Ti₂AlC 在 1000~1200 ℃ Ar-41% H₂O 气氛中的氧化行为。研究结果表明: 随着 Al 含量的减少, Ti₂AlC 在高温水蒸气中的氧化动力学由抛物线规律向线性规律转变; 当 Al 含量不足时, 连续氧化铝层的生长受到限制, 形成了不具备保护性的 TiO₂ 基氧化层; 近化学计量比的 Ti₂AlC 表面可生成较薄的连续致密 Al₂O₃ 层, 防止水蒸气向基体内的扩散。因此, 采用近化学计量比的 Ti₂AlC 作为锆合金表面的防护涂层时, 能够在高温水蒸气的环境下保护包壳, 提升现有轻水反应堆事故容错的能力。

**关 键 词:** 事故容错燃料; Ti₂AlC; 高温水蒸气氧化

**中图分类号:** TQ174　　**文献标志码:** A